Rates and processes affecting As speciation and mobility in lake sediments during aging

Alan Lock[1],*, Dirk Wallschläger[2], Nelson Belzile[3], Graeme Spiers[4], Celine Gueguen[5]

1. Environmental and Life Sciences Graduate Program, Trent University, Peterborough, Ontario, Canada
2. School of the Environment, Department of Chemistry and Water Quality Centre, Trent University, Peterborough, Ontario, Canada
3. Department of Chemistry, Laurentian University, Sudbury, Ontario, Canada
4. School of the Environment, Departments of Earth Sciences and Biology, Laurentian University, Sudbury, Ontario, Canada
5. School of the Environment and Chemistry Department, Trent University, Peterborough, Ontario, Canada

ARTICLE INFO

ABSTRACT

Sediments from an arsenic (As) contaminated groundwater vent site were used to investigate As(III) binding, transformation and redistribution in native and iron oxide amended lake sediments using aging spiked batch reactions and a sequential extraction procedure that maintains As(V) and As(III) speciation. In the native sediments, fractionation analysis revealed that 10% of the spiked As(III) remained intact after a 32-day aging experiment and was predominantly adsorbed to the strongly sorbed ($NH_4H_2PO_4$ extractable) and amorphous Fe oxide bound (H_3PO_4 extractable) fractions. Kinetic modelling of the experimental results allowed identifying the dominant reaction path for depletion of dissolved As(III) to As(III) absorbed on to the solid phase, followed by oxidation in the solid phase. Arsenite was initially adsorbed primarily to the easily exchangeable fraction (($NH_4)_2SO_4$ extractable), then rapidly transformed into As(V) and redistributed to the strongly sorbed and amorphous Fe oxide bound fractions. Oxidation of As(III) in recalcitrant fractions was less efficient. The iron oxide amendments illustrated the controls that iron oxides can have on As(III) binding and transformation rates. In goethite amended samples As(III) oxidation was faster and primarily occurred in the strongly sorbed and amorphous Fe oxide bound fractions. In these samples, 19.3 μg Mn was redistributed (compared to the native sediment) from the easily exchangeable and crystalline Fe oxide bound fractions to the strongly sorbed and amorphous Fe oxide bound fractions, indicating that goethite may act as a catalyst for Mn(II) oxidation, thereby producing sorbed Mn(III/IV), which then appears to be involved in rapidly oxidizing As(III).

© 2017 The Research Center for Eco-Environmental Sciences, Chinese Academy of Sciences. Published by Elsevier B.V.

Introduction

Arsenic, a known carcinogen (Morton and Dunnette, 1994), is found in many environments including rivers, lakes, groundwater, sediments, soils, mineral deposits, and tailings (Nicholas et al., 2003; Smedley and Kinniburgh, 2002). It is a major component of more than 200 minerals, including elemental arsenic, sulphides, oxides, arsenate (As(V)), and arsenite (As(III)) (Smedley and Kinniburgh, 2002). The reduced As species (As(III)) is often more mobile and toxic than As(V) (Coddington, 1986). It is generally accepted that in oxic environments, As(V) is sorbed to Fe oxides and oxyhydroxides (Hudson-Edwards et al., 2004; Jacobs et al., 1970; Matera et al., 2003; Montperrus et al., 2002; Smedley and Kinniburgh, 2002). However, As(III) binds to Fe

* *Corresponding author.* E-mail: alock@laurentian.ca (Alan Lock).

oxides and hydroxides too (Dixit and Hering, 2003; Manning et al., 1998; Manning and Suarez, 2000; Masscheleyn et al., 1991). In dynamic environments As can be transported across redox gradients, for example from reducing groundwater to oxidizing soils/sediments. Environmental changes can alter the redox potential of arsenic-bearing sediment layers, and thereby alter As mobility. For example decreasing near surface lake sediment redox potential from lake eutrophication could potentially cause reductive dissolution of Fe and Mn oxides, thereby releasing As species bound to such mineral fractions. Although reactions of As(III) with soils and sediments have been studied, rates and processes of As(III) transformation, adsorption and redistribution are still not well understood.

Edwards (1994) determined that As(III) oxidation in water may take days, weeks or months depending on the matrix. Arsenite oxidation in sediments is dominantly controlled by MnO_2 through heterogeneous reactions (Oscarson et al., 1983; Scott and Morgan, 1995; Sun and Doner, 1998) and Fe (oxy)hydroxides have been reported to oxidize As(III) as well (De Vitre et al., 1991). Huang et al. (1982) concluded that the rate limiting step for dissolved As(III) depletion (oxidation + adsorption) in sediment batch reactions is diffusion with kinetic rate constants (k) in the order of 10^{-2}/hr over a 24 hr period. Manning and Suarez (2000) conducted As(III) oxidation kinetic studies in soils illustrating that As(III) adsorption to Fe oxides and phyllosilicates increases with increasing pH, therefore decreasing As(III) availability for oxidation by MnO_2. At lower pH, As(III) oxidation by MnO_2 is more rapid and As(V) adsorption is faster and stronger. In synthetic goethite systems (pH 6.5 to 8.6) oxidation of adsorbed As(III) is shown to not occur over a 16 day period in wet and dry samples (Manning et al., 1998). However, Sun and Doner (1998) observed 10% to 20% As(III) oxidation in a goethite suspension after 100 hr at pH 5 and >20% oxidation of As(III) adsorbed on air dried goethite (pH 7) after 20 days. When birnessite (a mixed oxide of manganese and alkali) is added to the system most of the As(III) is oxidized within 1 hr.

Arsenic has been shown to bind to ferrihydrite surfaces through adsorption and not as a precipitate as revealed by similarities in extended X-ray absorption fine structure (EXAFS) data for As(V) and ferrihydrite co-precipitated *vs.* adsorbed samples (Fuller et al., 1993; Waychunas et al., 1993). Adsorption of As(III) is generally considered to be lower and weaker than As(V) at environmental pH because H_3AsO_3 has a neutral charge whereas As(V) is anionic at most pH (Manning and Martens, 1996). Manning and Goldberg (1997) showed that As(III) adsorption to clay minerals is much lower and weaker than for As(V). The adsorption rate for As has been described with two rate constants: k_1 (fast) and k_2 (slower) (Manning and Suarez, 2000; Huang et al., 1982). Proposed theories for the processes controlling these rates are high energy surface sites being available during early adsorption periods, but as these sites are occupied the slower process is limited by diffusion rate. Fuller et al. (1993) support this theory by fitting measured data to a diffusion–adsorption coupled model.

Manning and Suarez (2000) using $H_2PO_4^-$ extractions revealed dissolved As(III) depletion kinetics over a 48 hr period for two solid phase fractions with k_1 and k_2 constants on the order of 10^{-2} and 10^{-3}/hr, respectively. Fraction 1 identified depletion kinetics for the total reacted soil as revealed by

separation of As from the solution to soil and analysis of the supernatant. Fraction 2 identified As(III) and As(V) $H_2PO_4^-$ exchangeable depletion rates revealed by a $H_2PO_4^-$ extraction of the residual soil. This approach improves the understanding of the strength at which As can be immobilized over time because it quantitatively identifies an operationally defined fraction of the soil to which As binds. However, the authors can only speculate on the speciation and fate of the residual adsorbed fraction because they could not further extract As while maintaining the speciation.

Arsenite fractionation has not been extensively studied due to only recent development of sequential extraction procedures that maintain As(V) and As(III) speciation (Huang and Kretzschmar, 2010; Lock et al., 2016a). Application of fractionation analysis to aged samples revealing As(III) transformation and redistribution has not been conducted and will expand the understanding of As(III) transformation and complexing processes in environmental materials. The work of Manning and Suarez (2000) can be expanded beyond dissolved As and $H_2PO_4^-$ extractable As species to additional fractions, such as easily exchangeable, amorphous Fe oxide bound and crystalline Fe oxide bound. This will quantitatively improve the understanding of solid phase As(III) transformation and redistribution rates and processes.

Sun and Doner (1998) illustrate a box model similar to Fig. 1 depicting two possible reaction paths that As(III) may follow during transformation and adsorption of As(V) to a synthetic goethite. In one scenario As(III) is first adsorbed and then oxidized to As(V) in the solid phase (path $A_1 \rightarrow A_2$ here) and in the second scenario As(III) is first oxidized in solution and As(V) is then adsorbed (path $B_1 \rightarrow B_2$ here). Sun and Doner (1998) exclude path B as the likely process because the oxidation rate they observed on synthetic goethite was too fast to be attributed only to oxidation in the solution phase. Similarly, Manning and Suarez (2000) suggest that path A is the most likely process because they did not observe As(III) oxidation in KH_2PO_4 soil extract solutions. However, there are reports (Cherry et al., 1979; Early and Schramke, 1990; Edwards, 1994; Johnson and Pilson, 1975) of (slow) abiotic As(III) oxidation in waters, so the alternate pathway cannot be ruled out generally.

Since some uncertainties remain regarding solid phase As(III) transformation mechanisms and of the fate of recalcitrant As(III) during aging, and since the current knowledge on
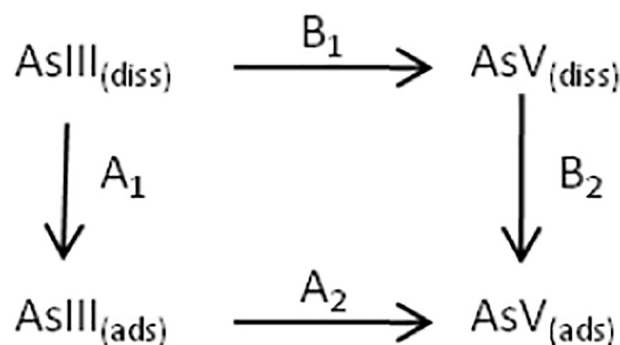

Fig. 1 – Possible reaction paths for As(III) in oxic sediment suspensions.

the As(III) adsorption and transformation reaction path lacks experimental verification, additional study of As(III) transformations, redistribution and processes is warranted. Therefore, expanding on the work Sun and Doner (1998) conducted using synthetic goethite and Manning and Suarez (2000) did with soils, we will determine in this study the dominant reaction path for As(III) adsorption and transformation to As(V) in lake sediments. The objectives of this study were: (1) to determine the dominant dissolved As(III) adsorption and oxidation reaction path and (2) to measure the redistribution and transformation of As(III) and As(V) in operationally defined easily exchangeable, strongly sorbed, amorphous Fe oxide bound and crystalline Fe oxide bound sediment fractions during a 32-day aging period.

1. Methods

1.1. Background

A system transporting groundwater containing As(III) across a redox gradient has been identified in Ramsey Lake, Sudbury, Ontario, providing an opportunity to study As(III) transformations, adsorption, redistribution, and processes. A groundwater vent site (site 2) transporting As through the sediment into the lake water has previously been identified using high resolution water quality monitoring 1 m above lake sediments (Lock et al., 2016b). Preliminary studies of the sediment at the groundwater vent site identify a solid phase As enrichment zone with the maximum at 4 cm below the sediment surface (Appendix A Fig. S1). At 5 to 7 cm below the sediment surface dissolved As(III) and As(V) are at a maximum concentration of 160 and 20 μg/L, respectively (Appendix A Fig. S2). These pore water concentrations decrease to 40 μg/L for As(III) and <0.2 μg/L (method detection limit) for As(V) by 2 cm below the sediment surface. These trends reveal that sediment sorption processes dominate from the first 2 to 5 cm below the sediment surface. Using the sediment surface area (30,000 m^2) with the minimum oxidation/reduction potential from this site identified by Lock et al. (2016b) to indicate the area of upwelling groundwater and the groundwater recharge rate (4 L/min) from a well intersecting a bedrock fracture identified to transport the As enriched groundwater (Lock et al., 2016b), a flow rate estimate can be calculated for the groundwater upwelling through the sediment of 0.56 cm/month. This indicates that upwelling groundwater residence time in the dominant As(III) sorption zone (2 to 5 cm) is *ca.* 5 months. Improving the understanding of how As(III) binds, transforms and redistributes (potentially to more strongly complexed forms) with time will indicate the susceptibility of this system to have deleterious water quality impacts.

1.2. Experimental

Lake sediments from an As-rich groundwater vent site in Ramsey Lake, Sudbury, Ontario were collected as a composite of the top 5 cm from several gravity cores. The site was selected to provide natural lake sediment with Fe and Mn oxides reacting with As(III) and As(V), so experimental spikes are not foreign to the material and provide a response that may more closely match that of natural *in-situ* materials. In addition, the novel sequential extraction procedure (Lock et al., 2016a) used here was validated, in part, with this sediment. The composite sediments were homogenised, freeze dried, and disaggregated using a mortar and pestle. The sediment was separated into two batches using a riffle splitter. One batch was amended with 20% synthesized goethite (FeOOH) (pH 5.8 ± 0.8) to elucidate Fe oxide effects on As(III) adsorption, transformation and redistribution and the second batch was not amended (pH 4.8 ± 0.1). Goethite was synthesized following the methods of Schwertmann and Cornell (1991) and mineral identity confirmed with X-ray diffraction analysis.

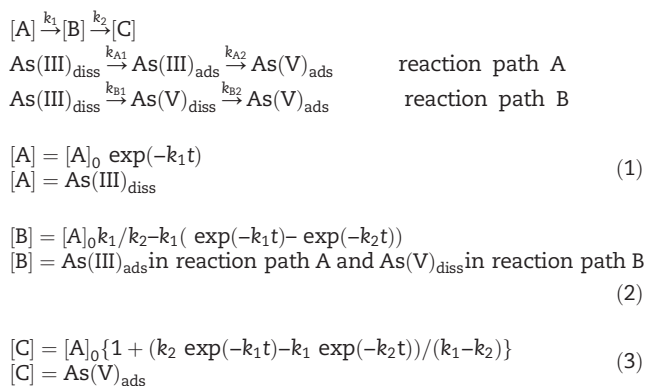Reactions of As(III) with the lake sediments were investigated in batch experiments using 50 mL polycarbonate centrifuge tubes. In each tube 0.4 g (±0.002 g) of sediment, either native or goethite amended were reacted with 25 mL of 10 mg/L (250 μg) As(III) or As(V) on a reciprocating shaker with tubes placed horizontally to maximize agitation for 0.3, 1, 2, 4, 8, 16, and 32 days. All sample treatments were processed in triplicate with averages being reported. Reactions were quenched by centrifuging (3000*g*, 15 min) and decanting the supernatant. An aliquot of the supernatant was diluted 100 times in a 2% HNO$_3$ solution and stored at 4°C for analysis using inductively coupled plasma mass spectrometer (ICP-MS) to provide data for total As and Mn concentrations. A second aliquot of the supernatant was used immediately after centrifuging to determine As(III) concentration following the solvent extraction method of Kamada (1976) and then back extracted into 25% HNO$_3$ (Balasoiu et al., 2001), diluted 10 fold and stored at 4°C for As analysis using ICP-MS. The solids remaining in the test tubes were sequentially extracted following the method of Lock et al. (2016a). This sequential extraction procedure was modified from Wenzel et al. (2001) to maintain As(V) and As(III) speciation and validated for the Ramsey Lake sediment using spike recoveries (Lock et al., 2016a). Operationally defined fractions targeted include easily exchangeable ((NH$_4$)$_2$SO$_4$), strongly sorbed (NH$_4$H$_2$PO$_4$), amorphous Fe oxides (H$_3$PO$_4$), crystalline Fe oxides (oxalate buffer, pH 3.25, 90°C), and residual (multi-step digest using HCl, HNO$_3$ and HF, 110°C). Supernatants from the sequential extractions were analysed for As(III), total As and Mn following the same procedures described above for the batch reaction supernatant samples.

Analytical grade standards of NaAsO$_2$ and Na$_2$HAsO$_4$·7H$_2$O were dissolved to make 1000 mg/L stock solutions of As(III) and As(V), respectively. Stock solutions were stored for no longer than 1 month at 4°C and working standard solutions were prepared and tested daily. Extracting reagents were prepared daily by dissolving analytical grade (NH$_4$)$_2$SO$_4$, NH$_4$H$_2$PO$_4$, NH$_4$OH·HCl, NH$_4$-oxalate, ascorbic acid, ethylenediaminetetraacetic acid, and ammonium pyrrolidinedithiocarbamate (APDC) in ultra pure water and reagent grade H$_3$PO$_4$, HNO$_3$, HF, and MIBK.

1.3. Kinetic model

As(III) oxidation in the sediment–water system is hypothesised to follow either path A, adsorption to the sediment followed by solid phase oxidation, or path B (Fig. 1), oxidation in solution followed by As(V) adsorption to sediment. Experiments that isolate the processes in reaction path for oxidation of As(III) in

solution and As(V) adsorption to the sediment were conducted to determine rate constants k_{B1} and k_{B2} values, respectively. The experimental data used to calculate k_{B1} for the oxidation of dissolved As(III) to As(V) in solution was determined using supernatant from Ramsey Lake sediment extracted for 16 hr with 0.05 mol/L $NH_4H_2PO_4$. Extraction with $NH_4H_2PO_4$ has been shown to liberate strongly sorbed As due to phosphate being smaller and having a higher charge density than arsenate (Wenzel et al., 2001), thus the extracted solution is expected to contain similar dissolved constituents that As may react with from the dissolved fraction of the batch reaction suspensions. The extract solution was spiked with 40 µg/L As(III) and aged in the dark at 20°C for 4 days. Subsamples taken at 0, 1, 2, 3, and 4 days were analysed for As(III) and As(V) using high performance liquid chromatography (HPLC) coupled to ICP-MS (Wallschlager and Stadey, 2007). The experimental data used to calculate k_{B2} for the adsorption of dissolved As(V) to sediment isolated from As(III) oxidation was determined using batch reactions with 25 mL of 10 mg/L As(V) solution mixed with 0.4 g of sediment shaking for 0, 0.3 and 1 days. The supernatant was analysed for As(III) and As(V) using HPLC–ICP-MS. Pseudo first order kinetic rate constants for k_{B1} and k_{B2} in reaction path B were calculated from the slope of a straight line fitted to the experimental data plotted as the change in ln[As] *vs.* time. Transformation, adsorption and redistribution were modelled following consecutive reaction paths A and B and kinetic reaction Eqs. (1) to (3) (Schnoor, 1996). The goodness of fit for modelled data to measured data was used to identify the dominant reaction path.

$$[A] \xrightarrow{k_1} [B] \xrightarrow{k_2} [C]$$

$$\text{As(III)}_{diss} \xrightarrow{k_{A1}} \text{As(III)}_{ads} \xrightarrow{k_{A2}} \text{As(V)}_{ads} \qquad \text{reaction path A}$$

$$\text{As(III)}_{diss} \xrightarrow{k_{B1}} \text{As(V)}_{diss} \xrightarrow{k_{B2}} \text{As(V)}_{ads} \qquad \text{reaction path B}$$

$$[A] = [A]_0 \exp(-k_1 t)$$
$$[A] = \text{As(III)}_{diss} \tag{1}$$

$$[B] = [A]_0 k_1 / k_2 - k_1 (\exp(-k_1 t) - \exp(-k_2 t))$$
$$[B] = \text{As(III)}_{ads} \text{ in reaction path A and As(V)}_{diss} \text{ in reaction path B} \tag{2}$$

$$[C] = [A]_0 \{1 + (k_2 \exp(-k_1 t) - k_1 \exp(-k_2 t))/(k_1 - k_2)\}$$
$$[C] = \text{As(V)}_{ads} \tag{3}$$

2. Results/discussion

2.1. Batch reactions and consecutive reaction model revealing dissolved As(III) fate and reaction path

Batch reactions spiked with 250 µg As(III) revealed an initial rapid depletion (oxidized + adsorbed) of dissolved As(III) during the first day (30%), followed by slower continued depletion for the 32 days reaction period (Fig. 2). The rapid depletion during the first day is from As(III) adsorption and subsequent oxidation to As(V) (14.4%), depicted as As(V)$_{(ads)}$, As(III) adsorption (6.9%) and As(III) oxidation in solution and/or at the sediment surface and released back to solution, depicted as As(V)$_{(diss)}$ (8.7%). Depletion of dissolved As(III) proceeding with two different rate constants, an initial fast k_1, followed by a slower k_2 matches
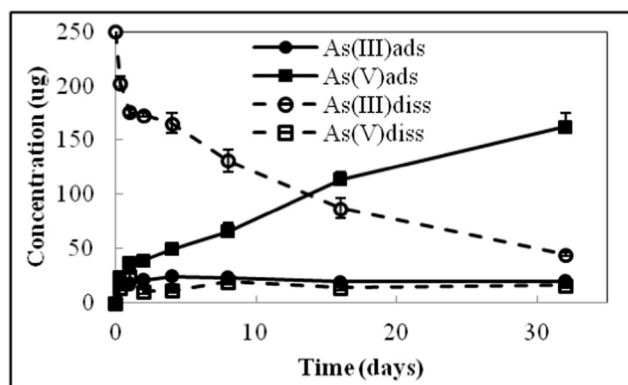

Fig. 2 – Adsorbed (ads) (sum of sequential extraction procedure fractions 1–4) and dissolved (dis) As(III) and As(V) partitioning in 250 µg As(III) spike batch reactions ($n = 3$).

what other studies have reported (Huang et al., 1982; Manning and Suarez, 2000). The initial fast reaction is attributed to high energy surface sites being occupied during early adsorption periods, but as these sites become saturated, Fuller et al. (1993) have shown that the slower depletion rate process (k_2) is limited by diffusion rate. Manning and Suarez (2000) furthermore showed that some As(III) remains intact and can be extracted with phosphate, but could not determine its subsequent fate. Our method shows that it is primarily subsequent oxidation in the solid phase. As the dissolved As(III) concentration decreases, sorbed As(V) concentration increases as a near mirror image. By day 32, 70% of the spiked As(III) is sorbed as As(V) and approximately 10% of spiked As(III) is adsorbed and remained intact (Fig. 2).

The conversion of dissolved As(III) to adsorbed As(V), combined with the observation of lesser amounts of adsorbed As(III) and dissolved As(V), identify two reaction paths that dissolved As(III) follows during aging with oxic sediment (Fig. 1). The presence of adsorbed As(III) (Fig. 2) revealed that some of the dissolved As(III) follows path A with dissolved As(III) being adsorbed, then oxidized in the solid phase. Similarly, measured dissolved As(V) revealed that some of the dissolved As(III) follows path B where As(III) is oxidized to As(V) in solution, followed by As(V) adsorption to the sediment. Because As(III)$_{ads}$ and As(V)$_{diss}$ remained nearly constant during the experiment and As(V)$_{ads}$ is significantly larger than either As(III)$_{ads}$ or As(V)$_{diss}$, k_1 must be the rate limiting step for the dominant reaction path. If k_2 was the rate limiting step, the concentration of As(III)$_{ads}$ or As(V)$_{diss}$ would increase with time until As(III)$_{diss}$ concentration is depleted. Huang et al. (1982) observed similar behaviour with As(III) oxidation and sorption occurring simultaneously.

Pseudo first order consecutive reaction models can be used to identify the dominant reaction path by comparing the fit between simulations and observed reaction kinetics. Using $NH_4H_2PO_4$ extracted sediment solution spiked with As(III) and aged for 4 days, an estimate of the pseudo first order rate constant for path B_1, oxidation of dissolved As(III) in solution, provides $k_{B1} = 0.023$/day ($R^2 = 0.78$) for path B_1. In a separate

batch reaction experiment, aging Ramsey Lake sediment with 250 μg As(V) revealed a pseudo first order rate constant of 0.9/day ($R^2 = 0.75$) for the depletion of dissolved As(V) that corresponds to the As(V) adsorption rate, reaction path B_2, supporting $k_{B2} > k_{B1}$ in reaction path B. Fig. 3a illustrates the disagreement between the measured values and model using these independently determined rate constants (path B_1 and path B_2). Therefore, path B is not likely the predominant reaction path because the rate constants determined for this reaction path do not produce a model simulation that matches the measured data. Fig. 3b shows the result of an optimization process that minimizes the variance between modelled and measured data from the 250 μg dissolved As(III) spiked batch reactions aged for 32 days, yielding rate constants for $k_{A1} = 0.06$/day and $k_{A2} = 0.3$/day. These constants do not match those determined experimentally for path B, and therefore apply to path A, with slower As(III) adsorption (k_{A1}) followed by more rapid oxidation (k_{A2}), which is the dominant path that immobilizes dissolved As(III).

Adsorption of As(III) followed by solid phase oxidation has previously been suggested (Manning and Suarez, 2000; Sun and

Fig. 3 – Pseudo first order consecutive reaction kinetic models depicting transformation, adsorption and redistribution for 250 μg dissolved As(III) mixed with 0.4 g of sediment.
(a) (path B) is constructed using k_{B1} data from measured As(III) oxidation in $NH_4H_2PO_4$ sediment extract solution (path B_1, $k_{B1} = 0.023$/day) and k_{B2} data from measured As(V) adsorption of 250 μg dissolved As(V) spike (path B_2, $k_{B2} = 0.9$/day).
(b) (path A) is constructed by fitting the model to measured data revealing best fits with $k_{A1} = 0.06$/day and $k_{A2} = 0.3$/day. Solid lines are measured data and dashed lines are modelled data.
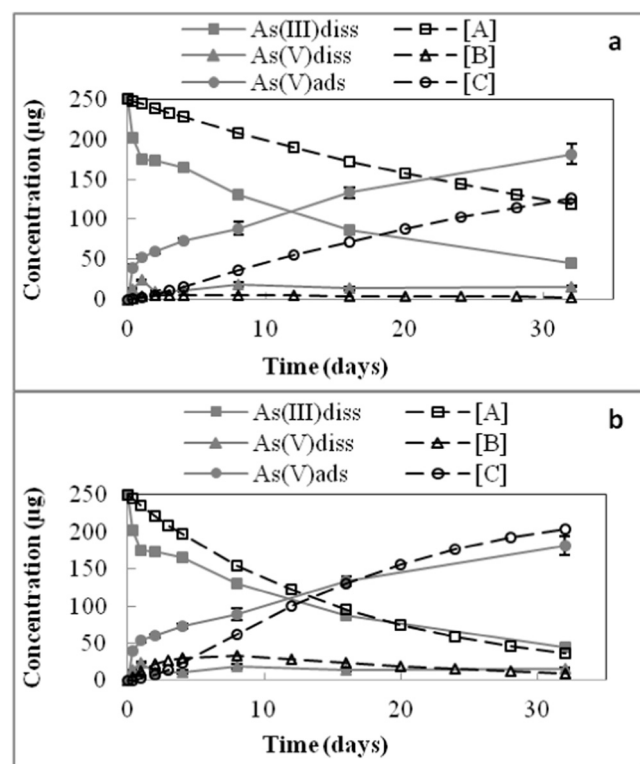
Doner, 1998), but validation with modelled data fit to measured values provides stronger evidence here. Sun and Doner (1998) suggest two plausible processes for rapid (birnessite assisted) solid phase oxidation of As(III): either (1) the goethite surface can act as a catalyst for Mn(II) oxidation by oxygen (Sung and Morgan, 1981), thus the newly formed Mn(III/IV) on the goethite surface can oxidize As(III) directly, or (2) colloidal and non-colloidal particle size fractions of MnO_2 may be active enough to oxidize the adsorbed As(III). Oscarson et al. (1981) reported that natural Mn oxides are present in both colloidal and non-colloidal particle size fractions. From the results obtained with Fe mineral amended sediments (see Section 2.3) there is evidence for process (1) occurring.

Path A (Fig. 3b) illustrates a weaker fit for initial time points, but a stronger fit for later time points (day 16 and 32). This reveals that from 0 to day 2 the reaction rate (k) is greater than used in the model, but after 2 days the kinetic coefficients used in the model (Fig. 3a) represent the measured data reasonably. Manning and Suarez (2000) observed similar trends for batch reactions with dissolved As(III) and soils aged for 2 days, concluding that the process is best described using a larger rate constant for early reaction periods and a smaller rate constant for the later part of the experiments. Fuller et al. (1993) showed *via* adsorption–diffusion coupled modelling that the faster depletion rate is controlled by available surface binding sites (k_1) and as these are increasingly occupied, interparticulate diffusion becomes rate limiting (k_2), decreasing the depletion rate. Hence, rate constants determined here that best simulate the later reaction period represent interparticulate diffusion rates.

2.2. Sequential extraction of As(III) spiked batch reactions

Arsenite concentration was largest in the amorphous Fe oxides followed by the strongly sorbed and easily exchangeable fractions, with the crystalline Fe oxides adsorbing the smallest concentration (Fig. 4a). Iron oxides have been identified as dominant adsorption sites for As(III) in oxic environments (Manning and Suarez, 2000). Amorphous Fe oxides have greater surface area and more binding sites than crystalline Fe oxides (Schwertmann et al., 1985), thus As(III) is expected to be predominantly complexed with this fraction (Deng and Stumm, 1994).

The As(III) concentration apex appeared first for the weakly sorbed fraction at 8 hr (6.3 μg). The As(III) concentration in this fraction decreased continuously after day 2. Concentration apexes in the more tightly bound fractions were observed later. Wang et al. (2015) observed similar trends for aged batch reactions spiked with As(V), with labile fractions complexing As first and redistribution to more refractory fractions during a 360 day aging experiment. During a 48 hr As(III) spiked aging experiment Manning and Suarez (2000) observed a decrease in total recoverable As (dissolved and PO_4 extractable) with time suggesting interparticulate diffusion of As(III) and As(V) to more recalcitrant fractions to account for the decrease. Without a sequential extraction procedure that maintains As speciation, the above aging experiments could not identify changes in As speciation for various fractions during redistribution. Here, As(V) and As(III) speciation, fractionation and redistribution of spiked As(III) are discussed for the first time.
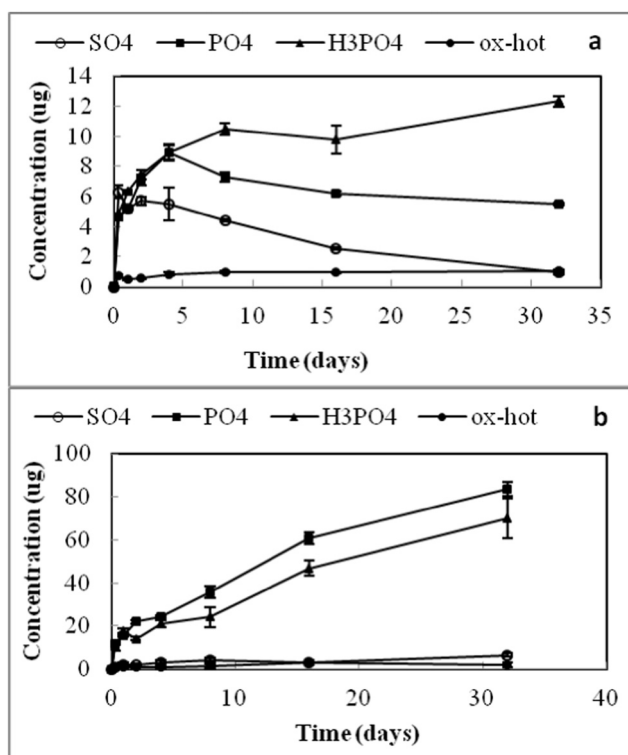
Fig. 4 – Arsenite (a) and arsenate (b) fractionation, transformation and redistribution for 250 μg As(III) spike in the native lake sediment (*n* = 3).

2.2.1. *Easily exchangeable ((NH$_4$)$_2$SO$_4$)*

The easily exchangeable As(III) fraction reached the peak value (6.3 μg) before all other fractions thus revealing the greatest adsorption rate during the first 8 hr compared to other fractions, but As(III) was consistently depleted from this fraction after 2 days. Hence, oxidation and redistribution must be greater than adsorption after 2 days. In the easily exchangeable fraction from day 2 to day 32, As(III) decreased by 4.3 ± 0.4 μg (Fig. 4a) and As(V) increased by 4.9 ± 0.7 μg (Fig. 4b), suggesting that the decrease in As(III) concentration for this fraction could be due to oxidation. However, Wang et al. (2015) observed a similar trend for aged batch reactions spiked with As(V) and showed that the As(V) decrease in loosely bound fractions is due to redistribution to more recalcitrant fractions. Similar trends were observed here for Ramsey Lake sediment aging batch reaction experiments spiked with As(V) (Appendix A Fig. S3). Hence, As(III) depletion from the easily exchangeable fraction may be due to oxidation and/or redistribution. Increasing As(V) concentrations in the strongly sorbed and amorphous Fe oxide bound fractions indicate that they must be the redistribution receptor fractions (Fig. 4b). In previous research, Dixit and Hering (2003) revealed that As(V) can be more strongly complexed than As(III) by observing greater concentrations of As(III) being extracted from Fe oxides using a phosphate extraction solution. Also, Wenzel et al. (2001) report evidence for the easily exchangeable fraction is complexed with outer-sphere bonds and the strongly sorbed fraction is complexed with inner-sphere bonds. Hence, oxidation of As(III) to As(V) likely

assists As redistribution from easily exchangeable outer-sphere bonds to strongly sorbed inner-sphere bonds.

The rate constant (*k*) for As(III) depletion from day 2 to day 16 in the easily exchangeable fraction was estimated at 0.06/day (R^2 = 0.99). This rate constant is the same as the k_{A1} rate constant (0.06/day) modelled for the As(III) loss from solution (Fig. 3b). This suggests that the dissolved As(III) depletion rate in water soils/sediment systems may be limited by the available surface adsorption sites in the easily exchangeable fraction. During the first two days, when large k_1 values best describe As(III) depletion, the easily exchangeable fraction increased most rapidly, representing many available surface reaction sites for this fraction being complexed. After 2 days, when the 0.06/day k_{A1} values best describes As(III) depletion, the initial reaction sites may be near saturation. In this stage, the rate is controlled by new sites that become available for adsorption as adsorbed As(III) is rapidly oxidized to As(V) in the easily exchangeable fraction, and redistributed to more tightly bound fractions through interparticulate diffusion. The easily exchangeable fraction outer-sphere bonds may represent sites for increased interaction of adsorbed As(III) with MnO$_2$, compared to more strongly complexed As(III), thus facilitating the most rapid As(III) oxidation in a solid phase. The easily exchangeable fraction complexes the greatest concentration of Mn^{2+} (see Section 2.3), likely as Mn(II). However, a rapid Mn(II) oxidation in this fraction is a plausible mechanism for As(III) oxidation here. In Section 2.3, evidence for rapid Mn(II) oxidation on goethite mineral surface is presented. Redistribution may be facilitated by As(III) forming weaker bonds than As(V), thus after oxidation, As(V) can be redistributed to the strongly sorbed and amorphous Fe oxide bound fractions. Although this fraction accounts only for a small portion of the adsorbed As, it may represent a very important portion of the sediment controlling As(III) oxidation and redistribution, as indicated by similar rate constants for dissolved As(III) depletion and As(III) oxidation and redistribution from the easily exchangeable fraction to more strongly bound fractions.

2.2.2. *Strongly sorbed (NH$_4$H$_2$PO$_4$)*

In the strongly sorbed fraction, from the concentration peak (day 4) to day 32, As(III) decreased by 3.4 μg (Fig. 4a) and As(V) increased by 59 μg (Fig. 4b). The rate constant for the decrease of adsorbed As(III) in the strongly sorbed fraction from day 4 to day 32 was estimated at 0.014/day (R^2 = 0.84). The rate constant for net increase of As(V) adsorbed to the strongly sorbed fractions was estimated at 0.041/day (R^2 = 0.89), illustrating that As(III) depletion from the strongly sorbed fraction is slower than As(V) accumulation in the strongly sorbed fraction. Hence, increasing concentration of As(V) in the strongly sorbed fraction is then mostly from As(III) oxidized in the easily exchangeable fraction and redistributed as As(V) to the strongly sorbed fraction. Observed As(III) complexed to the strongly sorbed fraction that peaks in concentration at day 4 indicates that this fraction also oxidizes As(III). However, the larger rate constant for As(III) depletion from the easily exchangeable fraction (0.06/day) compared to As(III) depletion from the strongly sorbed fraction (0.014/day) and As(V) increase in concentration for the strongly sorbed fraction (0.041/day) indicates that As(III) is mostly oxidized in the easily exchangeable fraction and then

redistributed as As(V) to the strongly sorbed fraction. Literature (Fuller et al., 1993; Huang et al., 1982; Manning and Suarez, 2000) reports that interparticulate diffusion controls As adsorption rate. Having identified As reaction rates to be diffusion controlled, we note that diffusion from the easily exchangeable fraction was greater than diffusion from the strongly sorbed fraction, in accordance with the relative accessibility of As in these fractions.

2.2.3. Amorphous Fe oxides (H_3PO_4)

The adsorbed As(III) concentration in the amorphous Fe oxide bound fraction increased for the duration of the experiment (Fig. 4a), revealing that oxidation of As(III) complexed to this fraction is less efficient compared to the more labile fractions. After the 32 day experiment, 14% of the As adsorbed to native sediments remained as As(III), and most of it was associated with the amorphous Fe oxide fraction. Arsenite has been shown to remain intact on certain mineral surface sites, especially Fe oxides (Manning et al., 1998). In contrast, De Vitre et al. (1991) report that natural and synthetic Fe oxyhydroxides oxidized 50% to 75% of added As(III) within 2 days. Samples amended with Fe oxides (see Section 2.3) revealed greater oxidation of added As(III) compared to native samples, partially in the amorphous Fe oxide bound fraction, hence demonstrating that some of the As(III) complexed with this fraction was oxidized, while a portion may remain intact. Arsenate complexed by the amorphous Fe oxide bound fraction increased for the duration of the experiment similar to As(V) complexed to the strongly sorbed fraction (Fig. 4b). This increase is attributed to As(III) oxidation directly in this fraction and As(V) redistribution from labile fractions.

2.2.4. Crystalline Fe oxides (oxalate buffer + ascorbic acid + heat)

Both As(V) and As(III) were extracted in the crystalline Fe oxide bound fraction, but only in very small amounts (Fig. 4a and b). Arsenite does not appear to have been oxidized in this fraction during the 32 day batch reactions as indicated by relatively constant concentrations for As(III) and As(V) for the duration of the experiment. Arsenic association with this fraction may be limited because surface reactions are possibly inhibited by other sediment fractions. Although it is likely that As is complexed by crystalline Fe oxides, such as goethite, fractionation results here revealed that As associated with these minerals was mostly released in earlier extraction steps. With further aging beyond the 32 day duration of this experiment, additional As is expected to redistribute to the crystalline Fe oxide bound fraction, similar to observations by Wang et al. (2015).

2.3. Amended samples

The above experiment using native samples illustrates As(III) fractionation, transformation and redistribution, but it does not elucidate controlling mechanisms, particularly for transformation. Previous research (Manning and Suarez, 2000) identified the concentration of Fe oxides as an important soil property influencing dissolved As(III) depletion, but there is a lack of consensus in the literature regarding the role of Fe oxides in As(III) oxidation. De Vitre et al. (1991) reported that

Fe oxyhydroxides oxidize 50% to 75% of As(III) in sediments within 2 days. Sun and Doner (1998) observed 10% to 20% As(III) oxidation in a goethite suspension after 100 hr (pH 5) and greater than 20% oxidation of As(III) on air dried goethite (pH 7) after 20 days. After adding birnessite, most of the As(III) oxidized in 1 hr. In contrast, Manning et al. (1998) showed no As(III) oxidation by synthetic goethite occurred over 16 days for wet and dry samples (pH 6.5 to 8.6). Manning and Suarez (2000) observed that as pH increased, As(III) adsorption to Fe oxides increased and oxidation decreased. Fractionation analysis of As(III) spiked batch reaction experiments using Fe oxide amended Ramsey Lake sediment may be able to determine further how Fe oxides impact As(III) depletion rates, transformation and fractionation. Hence, native sediment was amended with 20% synthetic goethite and used for batch reaction experiments similar to the native sediment experiments. Goethite, a crystalline Fe oxide, was mostly extracted with heated oxalate + ascorbic acid in the step referred to as crystalline Fe oxide bound.

The goethite amended samples depleted dissolved As(III) by day 8 (Appendix A Fig. S4), whereas the native samples did not deplete all of the 250 µg dissolved As(III) spike after 32 days, with 18% remaining in solution as As(III) (Fig. 2). The Fe oxide amended samples oxidized more of the As(III) compared to the native samples. With 18% of the original As(III) spike remaining dissolved at the 32 day reaction period the native samples oxidized 67% of the total As(III) (Fig. 2), whereas the goethite amended samples oxidized 90% (Fig. 5).

Goethite amended samples adsorbed most of the As(III) to the strongly sorbed and amorphous Fe oxide bound fractions where As(III) was rapidly oxidized as indicated by the decrease of As(III) and corresponding increase of As(V) in the same fractions (Fig. 5). Because the As(V) concentration in the amorphous Fe oxide bound fraction increased more rapidly than the As(III) concentration decreased, there must be another source of As(V). After 8 days, As(V) in the strongly sorbed fraction decreased, revealing that As(V) was redistributed from this fraction to amorphous and crystalline Fe oxide fractions. The strongly sorbed fraction here appears to have similar oxidation and redistribution rate controlling properties as observed for the easily exchangeable fraction in the native samples. The different fractions controlling reaction rates for native vs. amended samples illustrate that increased Fe oxide concentration changes the dominant fraction where As is initially complexed and oxidized to one that is more strongly bound. This can be expected because Fe oxide concentration has been shown to be an important soil characteristic controlling As(III) adsorption (Manning and Suarez, 2000). Fig. 5a reveals that the crystalline Fe oxide bound fraction does not contribute to As(III) oxidation, but does accumulate As(V) (Fig. 5b) through redistribution from other fractions.

Arsenite was oxidized most rapidly in the goethite amended samples, but oxidation was not observed in the fraction where goethite was most likely extracted (crystalline Fe oxide bound fraction) indicating that As(III) was complexed by surface adsorption. This matches observations by Keon et al. (2001), who extracted most of the As adsorbed on synthetic goethite using orthophosphate (phosphate), confirming that As associated with goethite should extract in steps 2 and 3 of our SEP, as seen in Fig. 5, where the accumulation of As(V) was observed
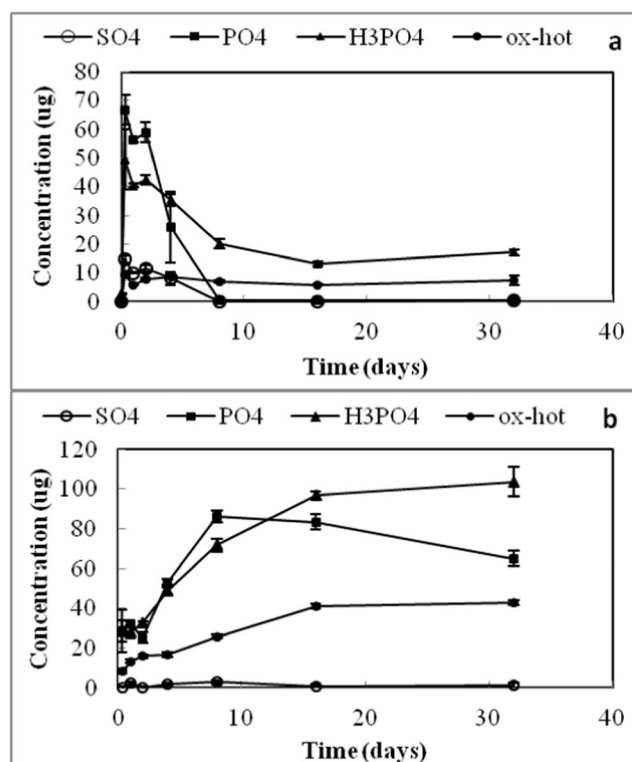
Fig. 5 – Arsenite (a) and arsenate (b) fractionation, transformation and redistribution for 250 μg As(III) spike in the goethite amended lake sediment (*n* = 3).
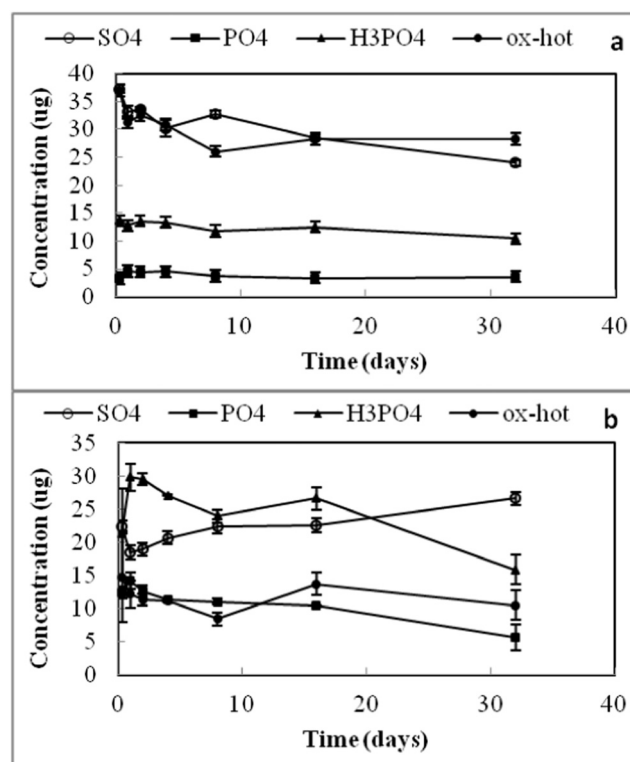

Fig. 6 – Manganese fractionation, transformation and redistribution for native (a) and goethite amended (b) lake sediment (*n* = 3) spiked with As(III).

during aging. Therefore, we can conclude that goethite itself does not appear to oxidize the As(III) bound to it.

Instead, goethite amendment altered the Mn fractionation compared to the native samples (Fig. 6), most likely indirectly facilitating As(III) oxidation. The most notable differences for the goethite amended samples (Fig. 6b), compared to the native samples (Fig. 6a), are increased Mn concentrations in the strongly sorbed and amorphous Fe oxide bound fractions with a decrease in the crystalline Fe oxide bound fraction. In Fig. 5 we observe the greatest evidence for As(III) oxidation in the same fractions, strongly sorbed and amorphous Fe oxide bound. Sung and Morgan (1981) report that the goethite surface can act as a catalyst in the oxidation of Mn(II) by oxygen, thus providing Mn(III) and Mn(IV) that can oxidize As(III). From the fractionation results obtained here, it appears that Mn fractionates to the strongly sorbed and amorphous Fe oxide bound portions of the sediment under the influence of crystalline Fe (oxy)hydroxides, like goethite, and causes As(III) oxidation in these sediment fractions.

Lafferty et al. (2010) have shown that the oxidation of As(III) by MnO_2 produces As(V) and Mn(II), where Mn(II) can occupy sites on remaining MnO_2 surfaces passivating the As(III) oxidation reactions by competing for reaction sites. The As(III) oxidation reaction by MnO_2 must be considered as a potential mechanism controlling the observed Mn redistribution resulting in increased Mn concentrations in the strongly sorbed and amorphous Fe oxide bound fractions of the goethite amended samples (Fig. 6b) compared to native samples (Fig. 6a). In parallel

batch reaction experiments to the above amended sediments spiked with As(III), amended sediments were spike with As(V) (Appendix A Fig. S5). Comparison of the amended sediments spiked with As(III) (Fig. 6) and those spiked with As(V) (Appendix A Fig. S5) reveals similar Mn fraction. Hence, As(III) oxidation by MnO_2 is not the dominant process controlling the increased Mn concentrations observed in the strongly sorbed and amorphous Fe oxide bound fractions of the goethite amended samples. This further supports that the proposed controlling mechanism for increased As(III) oxidation in goethite amended samples is the goethite surface acting as a catalyst in the oxidation of Mn(II) by oxygen, thus providing Mn(III) and Mn(IV) that can oxidize As(III).

2.4. Ramsey sediment

The contact time estimate for the upwelling groundwater and most reactive part (indicated by maximum solid phase As concentration and depletion of dissolved As) of the solid phase As enrichment zone (2 to 5 cm below sediment surface) of the sediment was *ca.* 5 months (150 days). At the end of the 32-day laboratory experiments, 18% of dissolved As(III) remained in solution. Using the consecutive reactions model to predict the time required for complete removal of dissolved As(III) from solution was 120 days. This suggests that the current system is not contaminating the surface water. However, water sampled directly above the sediment at the groundwater vent site contained 12 μg/L dissolved As (Lock et al., 2016b), corresponding to 7% of the upwelling dissolved As not being adsorbed. This

is in reasonable agreement with the model prediction, especially considering the simplistic methods used to estimate an approximate residence contact time for the upwelling water with the sediment.

Lake eutrophication has the greatest potential to mobilize As bound to the sediment in Ramsey Lake. Martin and Pedersen (2002) observed larger flux of dissolved As from lake sediment as primary production increased in Balmer Lake, Ontario. The larger flux was attributed to an increase of organic matter deposition that degraded, decreasing the redox potential at the sediment surface, thus increasing reductive dissolution of Fe and Mn oxides and mobilizing As. Elevated ion activity and particularly phosphate ions in the groundwater system transporting As may directly compete with As for binding sites in sediments. Phosphate has been used to extract strongly sorbed As from soils because the smaller size and greater charge density compete for binding sites with As (Wenzel et al., 2001). Results from the SEP suggest that As(III) oxidation is dominantly controlled by adsorption to the easily exchangeable and strongly sorbed fractions. If other ions compete for these adsorption sites As(III) adsorption and oxidation rate may decrease.

3. Conclusions

Understanding As(III) binding, redistribution and transformation within soils and sediments is an important part of managing arsenic in some environments, and thereby protecting human and ecological health. The research here confirms that As(III) oxidation in (sub)oxic soils and sediments follows a reaction path where As(III) is first adsorbed to the substrate, and then subsequently oxidized to less mobile As(V); thus, geochemical conditions encouraging As adsorption are beneficial. Adsorption and oxidation of As(III) is most rapid (hrs to 1 day) in the labile sediment fraction, which is followed by redistribution to more recalcitrant fractions. Competing ions, such as chloride or phosphate from urban or agricultural runoff, may interfere with As(III) adsorption to labile sediment fractions, thus increasing As(III) mobility and toxicity. Arsenite that is complexed by the recalcitrant fraction is less susceptible to oxidation, therefore Fe oxide substrates may retain a greater percentage of adsorbed As(III) over a system with a slower adsorption rate and higher oxidation efficiency. However, goethite was shown here to facilitate rapid As(III) oxidation, with evidence that the oxidation is driven by Mn(III/IV) generated in more available sediment fractions than goethite itself. Observations indicate that goethite may act as a catalyst for Mn(II) oxidation, thereby producing sorbed Mn(III/IV), which is then involved in rapidly oxidizing As(III). This should be confirmed with additional experiments conducted in a closed system using MnO_2 + FeOOH + As(III).

The consecutive reaction model is in close agreement with water quality data observed directly above the groundwater vent site in Ramsey Lake suggesting that our experiments represent environmental conditions satisfactorily. The upwelling site system is likely to become a source of As contamination if Ramsey Lake turned eutrophic, or if the groundwater system became enriched in phosphate. To better understand possible deleterious impacts from the sediment being exposed to increased phosphate concentrations competitive ion tests with the lake sediment, dissolved phosphate and dissolved As should be conducted.

Appendix A. Supplementary data

Supplementary data to this article can be found online at http://dx.doi.org/10.1016/j.jes.2017.05.003.

R E F E R E N C E S

Balasoiu, C., Zagury, G., Deschenes, L., 2001. Partitioning and speciation of chromium, copper, and arsenic in CCA-contaminated soils: influence of soil composition. Sci. Total Environ. 280, 239–255.

Cherry, J., Shaikh, A., Tallman, D., Nicholson, R., 1979. Arsenic species as an indicator of redox conditions in groundwater. J. Hydrol. 43, 373–392.

Coddington, K., 1986. A review of arsenicals in biology. Toxicol. Environ. Chem. 11, 281–290.

De Vitre, R., Belzile, N., Tessier, A., 1991. Speciation and adsorption of arsenic on diagenetic iron oxyhydroxides. Limnol. Oceanogr. 36 (7), 1480–1485.

Deng, Y., Stumm, W., 1994. Reactivity of aquatic iron (III) oxyhydroxides — implications for redox cycling of iron in natural waters. Appl. Geochem. 9 (1), 23–36.

Dixit, S., Hering, J.G., 2003. Comparison of arsenic(V) and arsenic(III) sorption onto iron oxide minerals: implications for arsenic mobility. Environ. Sci. Technol. 37 (18), 4182–4189.

Early, L.E., Schramke, J.A., 1990. Rates of inorganic oxidation reactions involving dissolved oxygen. In: Melchoir, D.C., Bassett, R.L. (Eds.), Chemical Modeling of Aqueous Systems II. ACS Symp. Ser.Am. Chem. Soc., Wash., DC, pp. 379–396.

Edwards, M., 1994. Chemistry of arsenic removal during coagulation and Fe–Mn oxidation. J. Am. Water Works Assoc. 86 (9), 64–78.

Fuller, C., Davis, J., Waychunas, G., 1993. Surface chemistry of ferrihydrite: part 2. Kinetics of arsenate adsorption and coprecipitation. Geochim. Cosmochim. Acta 57, 2271–2282.

Huang, J., Kretzschmar, R., 2010. Sequential extraction method for speciation of arsenate and asrenite in mineral soils. Anal. Chem. 82, 5534–5540.

Huang, P., Oscarson, D., Liaw, W., Hammer, U., 1982. Dynamics and mechanisms of arsenite oxidation by freshwater lake sediments. Hydrobiologia 91 (1), 315–3221.

Hudson-Edwards, K., Houghton, S., Osborn, A., 2004. Extraction and analysis of arsenic in soils and sediments. Trends Anal. Chem. 23 (10–11), 745–752.

Jacobs, L., Syers, J., Keeney, D., 1970. Arsenic sorption by soils. Soil Sci. Soc. Am. J. 34, 750–754.

Johnson, D.L., Pilson, M.E.Q., 1975. The oxidation of arsenite in sea water. Environ. Lett. 8, 157–171.

Kamada, T., 1976. Selective determination of arsenic (III) and arsenic (V) with ammonium pyrrolidinedithiocarbamate, sodium diethydithiocarbamate and dithizone by means of flameless atomic-absorption spectrophotometry with a carbon-tube atomizer. Talanta 23, 835–839.

Keon, N.E., Swartz, C.H., Brabander, D.J., Harvey, C., Hemond, H.F., 2001. Validation of an arsenic sequential extraction method for evaluating mobility in sediments. Environ. Sci. Technol. 35, 2778–2784.

Lafferty, B.J., Ginder-Vogel, M., Sparks, D.L., 2010. Arsenite oxidation by a poorly crystalline manganese-oxide 1. Stirred-flow experiments. Environ. Sci. Technol. 44, 8460–8466.

Lock, A., Wallschläger, D., McMurdo, C., Tyler, L., Belzile, N., Spiers, G., 2016a. Validation of an updated fractionation and indirect speciation procedure for inorganic arsenic in oxic and suboxic soils and sediments. Environ. Pollut. http://dx.doi.org/10.1016/j.envpol.2016.09.013.

Lock, A., Spiers, G., Hostetler, B., Ray, J., Wallschläger, D., 2016b. Multi-dimensional water quality assessment of an urban drinking water source elucidated by high resolution underwater towed vehicle mapping. Water Res. 93, 289–295.

Manning, B., Goldberg, S., 1997. Adsorption and stability of arsenic(III) at the clay mineral-water interface. Environ. Sci. Technol. 31, 2005–2011.

Manning, B., Martens, D., 1996. Speciation of arsenic(III) and arsenic(V) in sediment extracts by high-performance liquid chromatography-hydride generation atomic absorption spectrophotometry. Environ. Sci. Technol. 31, 171–177.

Manning, B., Suarez, D., 2000. Modeling arsenic (III) adsorption and heterogeneous oxidation kinetics in soils. Soil Sci. Soc. Am. J. 4, 128–137.

Manning, B.A., Fendorf, S.E., Goldberg, S., 1998. Surface structures and stability of arsenic (III) on goethite: spectroscopic evidence for inner-sphere complexes. Environ. Sci. Technol. 32, 2383–2388.

Martin, A., Pedersen, T., 2002. Seasonal and interannual mobility of arsenic in a lake impacted by metal mining. Environ. Sci. Technol. 36, 1516–1523.

Masscheleyn, P., Delaune, R., Patrick, H., 1991. Effects of redox potential and pH on arsenic speciation and solubility in a contaminated soil. Environ. Sci. Technol. 25, 1414–1419.

Matera, V., Le Hecho, I., Laboudigue, A., Thomas, P., Tellier, S., Astruc, M., 2003. A methodological approach for the identification of arsenic bearing phases in polluted soils. Environ. Pollut. 126, 51–64.

Montperrus, M., Bohari, Y., Bueno, M., Astruc, A., Astruc, M., 2002. Comparison of extraction procedures for arsenic speciation in environmental solid reference materials by high-performance liquid chromatography-hydride generation-atomic fluorescence spectroscopy. Appl. Organomet. Chem. 16, 347–354.

Morton, W., Dunnette, D., 1994. Health effects of environmental arsenic. In: Niragu, J. (Ed.), Arsenic in the Environment, Part II: Human Health and Ecosystem Effects. Wiley and Sons, Inc., New York, pp. 17–34.

Nicholas, D., Ramamoorthy, S., Palace, V., Spring, S., Moore, J., Rosenzweig, F., 2003. Biogeochemical transformations of arsenic in circumneutral freshwater sediments. Biodegradation 14, 123–137.

Oscarson, D., Rogers, J., Huang, P., Liaw, W., 1981. The nature of selected prairie lake and stream sediments. Int. Rev. Hydrobiol. 66, 95–107.

Oscarson, D., Huang, P., Liaw, W., Hammer, U., 1983. Kinetics of oxidation of arsenite by various manganese oxides. Soil Sci. Soc. Am. J. 47, 644–648.

Schnoor, J., 1996. Environmental Modeling: Fate and Transport of Pollutants in Water, Air, and Soil. John Wiley and Sons, Inc.

Schwertmann, U., Cornell, R.M., 1991. Iron Oxides in the Laboratory — Preparation and Characterization. VCH, New York 137.

Schwertmann, U., Cambier, P., Murad, E., 1985. Properties of goethite of varying crystallinity. Clay Clay Miner. 33 (5), 369–378.

Scott, M., Morgan, J., 1995. Reactions at oxide surfaces. I. Oxidation of As (III) by synthetic birnessite. Environ. Sci. Technol. 29, 1898–1905.

Smedley, P., Kinniburgh, D., 2002. A review of the sources, behaviour and distribution of arsenic in natural waters. Appl. Geochem. 17, 517–568.

Sun, X., Doner, H., 1998. Adsorption and oxidation of arsenite on goethite. Soil Sci. 163 (4), 278–287.

Sung, W., Morgan, J., 1981. Oxidative removal of Mn(II) from solution catalyzed by lepidocrocite surface. Geochim. Cosmochim. Acta 45, 2377–2383.

Wallschlager, D., Stadey, C.J., 2007. Determination of (oxy)thioarsenates in sulfidic waters. Anal. Chem. 79, 3873–3880.

Wang, Y., Zeng, X., Lu, Y., Su, S., Bai, L., Li, L., Wu, C., 2015. Effects of aging on the bioavailability and fractionation of arsenic in soils derived from five parent materials in a red soil region of Southern China. Environ. Pollut. 207, 79–87.

Waychunas, G., Rea, B., Fuller, C., Davis, J., 1993. Surface chemistry of ferrihydrite: part 1. EXAFS studies of the geometry of coprecipitated and adsorbed arsenate. Geochim. Cosmochim. Acta 57, 2251–2269.

Wenzel, W., Kirchbaumer, N., Prohaska, T., Stingeder, G., Lombi, E., Adriano, D., 2001. Arsenic fractionation in soils using an improved sequential extraction procedure. Anal. Chim. Acta 436, 309–323.